Proceedings of the
Annual Stability Conference
Structural Stability Research Council
Atlanta, Georgia, April 21-24, 2026

Elevated temperature tests on cold-formed steel members in compression: effect of member length, temperature profile, and heating regime

Jiangyue Xie[1], Thomas Gernay[2]

Abstract

This study focuses on elevated temperature testing of cold-formed steel members, whose behavior is influenced by the complex interaction of buckling modes, temperature degradation of properties, and thermally induced deformations and stresses. There remains a lack of experimental data on member-level behavior under various test conditions, including transient and non-uniform heating, with most available tests limited to steady-state uniform heating. In this study, a customized electric furnace was built to apply uniform and non-uniform temperature distributions at controlled rates on channel members loaded in compression. Tests on 600S200-54 lipped channels with length of 457 and 1219 mm were conducted under both steady-state and transient heating. The specimens were heated to temperatures ranging from 300 °C to 600 °C either uniformly or non-uniformly with a controlled 100 °C temperature gradient between flanges. The channels had measured axial strength of 101 kN and 81 kN for the short and long specimens, respectively; these strengths were reduced to approximately 30% of their original values at 600 °C under uniform heating. Under transient heating, the specimens loaded to 40% of their ambient capacity sustained temperatures of about 600 °C prior to failure, whereas those loaded to 85% failed at temperatures between 300 °C and 400 °C. Results from non-uniform heating tests showed that the hotter flange temperature at failure can exceed the critical temperature under uniform heating conditions. These test data provide benchmarks for advancing models and supporting the development of performance-based fire design for cold-formed steel structures.

1. Introduction

The use of cold-formed steel (CFS) assemblies is common in the United States for structural and non-structural application in low- and mid-rise buildings. Thin-walled CFS members' advantages include a high strength-to-weight ratio and rapid construction with ease of installation. For gravity load-bearing systems, closely spaced CFS framing members (commonly referred to as studs) are coupled with tracks and gypsum sheathing to form wall assemblies. However, CFS studs are susceptible to instability due to their thin-wall geometry. Common buckling modes include local, distortional, global (flexural, torsional), and their interactions. While extensive work has been conducted on the stability and axial capacity of CFS studs at ambient temperature (David *et al.* 2011, Tian *et al.* 2004, Zhang *et al.* 2025, Roy *et al.* 2019, Yap *et al.* 2011), experimental investigations under fire exposure remain relatively limited. Existing fire tests have largely focused on wall assemblies, where global buckling and failure modes have been observed (Chen *et al.* 2012,

[1] Ph.D. Candidate, Johns Hopkins University, <jxie47@jhu.edu>
[2] Associate Professor, Johns Hopkins University, < tgernay@jhu.edu >

Samiee *et al*. 2022, Abreu *et al.* 2020, Liu *et al.* 2024, Kesawan *et al.* 2015, Roy *et al.* 2019, Dias *et al.* 2019, Ariyanayagam and Mahendran 2014, Feng and Wang 2005). While these studies have generated valuable insights, the intrinsic behavior and capacity of individual studs are difficult to isolate due to complex interactions among studs, tracks, sheathing, and boundary conditions within assemblies. To address this limitation, some experimental studies have examined individual CFS studs, including steady-state tests on short studs under uniform heating (Gunalan *et al.* 2015, Feng *et al.* 2003, Ranawaka *et al.* 2009, Xie *et al.* 2025) and transient tests on long studs (Craveiro *et al.* 2016, Yang *et al.* 2023, Ali *et al.* 1998). However, there remains a need for additional data for a comprehensive understanding of stud behavior in wall assemblies where the studs are typically subject to non-uniform temperature distributions from one-sided fire exposure. Recent temperature measurements from compartment fire tests conducted on a 10-story CFS building at UCSD have allowed quantifying the non-uniform temperature distributions within wall assemblies under natural fire (CFS-NHERI 2025). These findings underscore the need for experimental data on individual CFS studs subjected to well-controlled uniform and non-uniform elevated temperatures. Such data are essential for developing reliable calculation methods and advancing performance-based structural fire design approaches that enhance both fire safety and design efficiency.

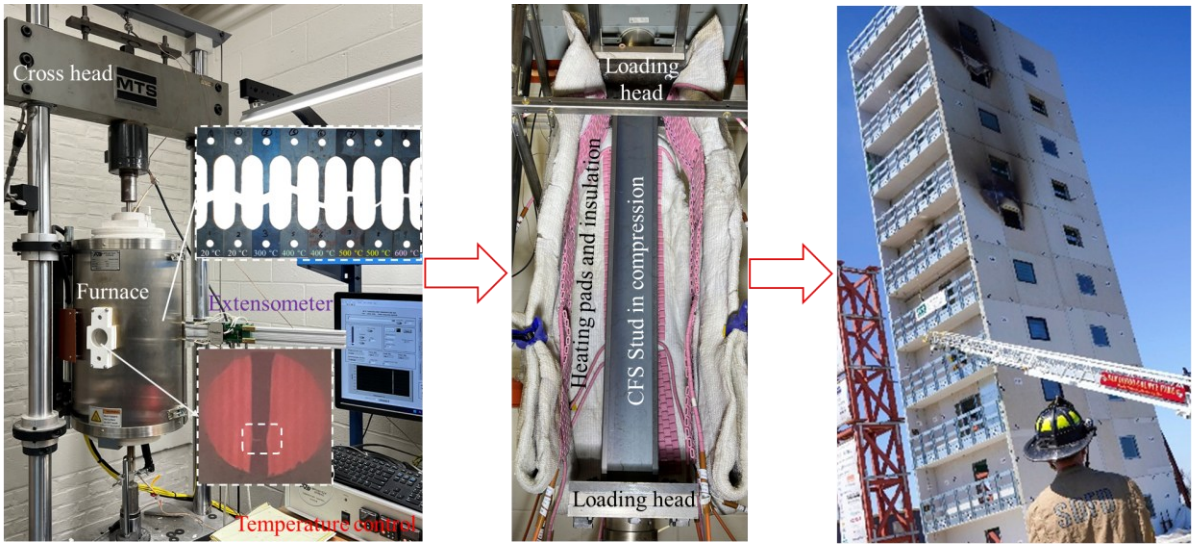

Test rig for the coupon tests | A channel stud installed in the test rig | 10-story building (cfs10.ucsd.edu)

Figure 1: Data collection effort on fire response of CFS structures across scales. This study describes experiments at the member level.

To collect the necessary data, an experimental effort across the material, member, and building scale is required, as illustrated in Figure 1. This study focuses on the member level and describes experiments conducted on single CFS studs; meanwhile the study leverages coupon data from material tests for material properties (Ma *et al.* 2025), and full-scale 10-story building fire test data to inform the thermal exposure used in the member experiments. A customized electric furnace was built within an MTS testing system to apply precisely controlled uniform and non-uniform temperatures on the specimens, creating thermal conditions representative of wall assemblies under realistic fires. Testing was conducted on 600S200-54 lipped channels in compression with lengths of 457 mm and 1219 mm in both steady-state and transient regimes. Specimens in steady-state tests were heated either uniformly to target temperatures ranging from 300 °C to 600 °C or non-uniformly with flange temperatures of 300-400 °C, 400-500 °C, and 500-600 °C. In transient

tests, studs were heated at a constant rate under either uniform temperature conditions or non-uniform heating with a 100 °C flange temperature gradient until failure, while sustaining axial load levels corresponding to 40% or 85% of their ambient-temperature capacities. In this study, test data was published on the DesignSafe website (Xie and Gernay 2025).

2. Experimental Method

2.1 Test rig and testing regimes

The experimental program was conducted in the Multi-Hazard Resilient Structures Laboratory at Johns Hopkins University. Tests were conducted with a mechanical loading system and heating system with independently controlled electric heating pads. The MTS machine has a capacity of 445 kN (100 kips) and can be operated either in force-control or displacement-control mode. The specimens were heated by independently controlled electric heating pads. To ensure thermal insulation and uniform load transfer, 25.4 mm thick insulation plates and 25.4 mm low-carbon steel plate were sandwiched on the loading head for insulation and load bearing. Both short and long studs were tested with bearing-bearing boundary conditions (B.C.). The test setup has been described (for the configuration for the 457 mm long studs) by Xie et. al. (2025). The configuration has been modified to accommodate 1219 mm long studs as shown in Figure 2. To securely support the thermocouples, two internal angle frames were bolted inside the furnace (visible in Figure 2(b)). These thermocouples were pressed against the stud surfaces which maintained consistent contact and reliable temperature measurements throughout the tests.

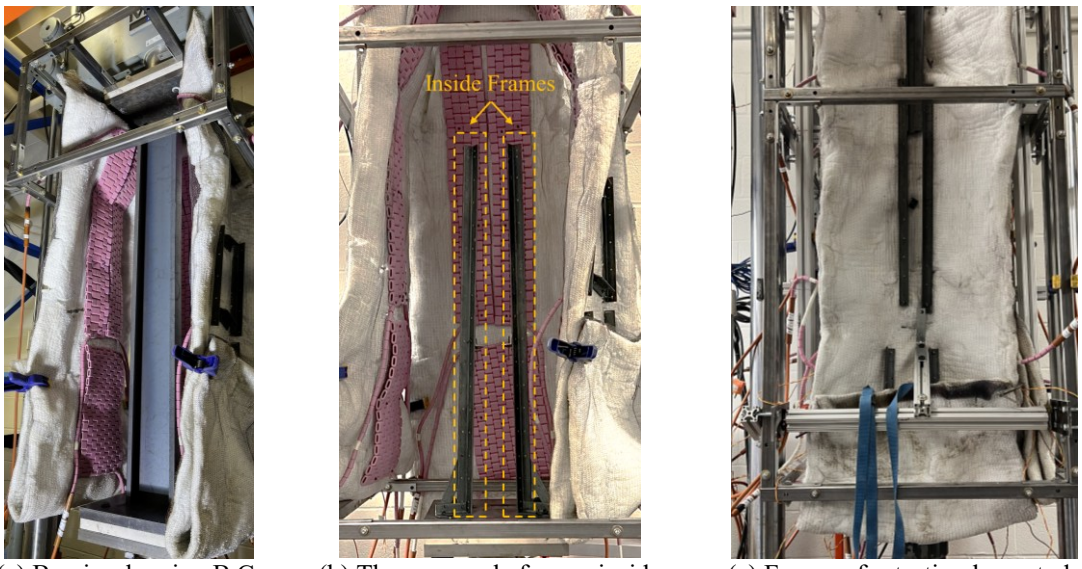

(a) Bearing-bearing B.C. (b) Thermocouple frames inside (c) Furnace for testing long studs

Figure 2: Boundary conditions, thermocouple frames, and insulation for the furnace in the “long” configuration

To generate controlled uniform and non-uniform thermal environments within the furnace, electrical heating pads were installed to form six independently controlled heating zones. These zones were arranged to apply heat to upper flanges, lower flanges, and web of stud specimens, as shown in Figure 3. The test area was wrapped with insulation blankets.

Both steady-state tests and transient tests were conducted. In steady state tests, specimens were first heated under either uniform or non-uniform temperature conditions to predefined target

temperatures. After heating and stabilization, axial loading was applied in displacement-control mode at a constant loading rate until failure. For non-uniform heating conditions, the temperature at the hotter side flange was maintained 100 °C higher than that at the less-heated side flange. Test outcomes included axial force-displacement curve at elevated temperature, from which the peak axial loads and strength retention factors can be derived. In contrast, transient tests followed a different heating-loading sequence. Specimens were initially loaded to either 85% or 40% of their ambient-temperature axial capacities and held under force-control mode. The studs were then heated, under either uniform temperature conditions or non-uniform conditions with a prescribed 100 °C flange temperature gradient, until failure occurred. During transient tests, critical temperatures to failure, heating rates, axial displacements, and buckling modes were recorded.

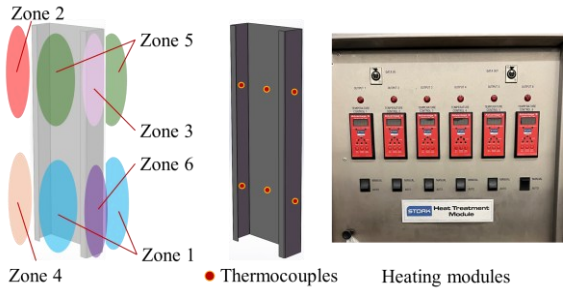

Figure 3: Heating zones, thermocouple locations, and heating modules

2.2 Test matrix and specimens

To investigate the axial capacity and buckling behavior of individual studs representative of those used in wall assemblies, 600S200-54 lipped channel studs with two different lengths were tested under both steady-state and transient fire conditions. Specimens with a length of 457 mm are further referred to as short studs, while those with a length of 1219 mm are long studs. In steady-state tests, specimens were heated uniformly to target temperatures of 300 °C, 400 °C, 500 °C, and 600 °C, or non-uniformly to prescribed flange temperature distributions of 300-400 °C, 400-500 °C, and 500-600 °C. These temperature levels were selected based on steel temperature measurements obtained from recent fire tests on a 10-story CFS building. As aforementioned, both short and long studs in transient tests were heated either uniformly or non-uniformly with 40% or 85% of their ambient capacities, corresponding to 0.40 and 0.85 initial utilization ratios. Each test was repeated twice for repeatability and reliability of the experimental results. All specimens were fabricated from low-carbon steel with a nominal yield strength of 345 MPa. The nominal cross-sectional dimensions of the studs are summarized in Table 1.

Table 1: Nominal dimensions of the 600S200-54 lipped channel studs

Web depth	Flange width	Stiffening lip	Fillet radius	Thickness	Length
152.4 mm	50.8 mm	15.875 mm	2.156 mm	1.438 mm	457.2 mm & 1219.2 mm
6 in.	2 in.	0.625 in.	0.0849 in.	54 mils	18 in. & 48 in.

Coupon tests were conducted under steady-state conditions at temperature of 300 °C, 400 °C, 500 °C, and 600 °C (ASTM 2009, ASTM 2016). Coupon specimens were cut from the web of the studs to characterize the material properties representative of the tested members. At ambient temperature, the elastic modulus was measured as 205,511 MPa, the yield strength determined using the 0.2% proof stress was 407 MPa, and the ultimate tensile strength was 462 MPa. The material properties obtained at elevated temperatures are summarized in Table 2.

Table 2: Measured material properties from the coupon tests on cold-formed steel

Num.	Temp. (°C)	E_T (MPa)	k_E (MPa)	$f_{u,t}$ (MPa)	k_u	$f_{y,0.2}$ (MPa)	$k_{y,0.2}$	$f_{y,2}$ (MPa)	$k_{y,2}$
1	20	205,511	1.000	462	1.000	407	1.000	405	1.000
2	300	175,634	0.855	435	0.942	326	0.801	383	0.946
3	400	111,597	0.543	336	0.726	269	0.382	306	0.756
4	500	99,785	0.486	229	0.496	196	0.278	221	0.545
5	600	41,243	0.201	121	0.262	123	0.175	120	0.296

Note: Temp. is uniformly elevated temperature in steady-state coupon tests.

2.3 Measured steel temperatures

A sample of temperatures measured on the steel specimens with K-type thermocouples is shown below. Figure 4(a) plots the steel temperature (average over the flanges and web) during steady-state tests under uniform elevated temperatures. The experimental setup can heat the specimen at a constant rate and then hold the temperature constant at the target elevated temperature.

Figure 4(b) shows the steel temperature recorded during transient tests under non-uniform heating conditions, controlled to maintain a 100 °C temperature gradient between the flanges. Again, the temperature measurements on the CFS channel show accurate control of the prescribed testing conditions. This confirms that the customized, multi-zone electrical heating system can be used to apply the desired thermal conditions on the specimen.

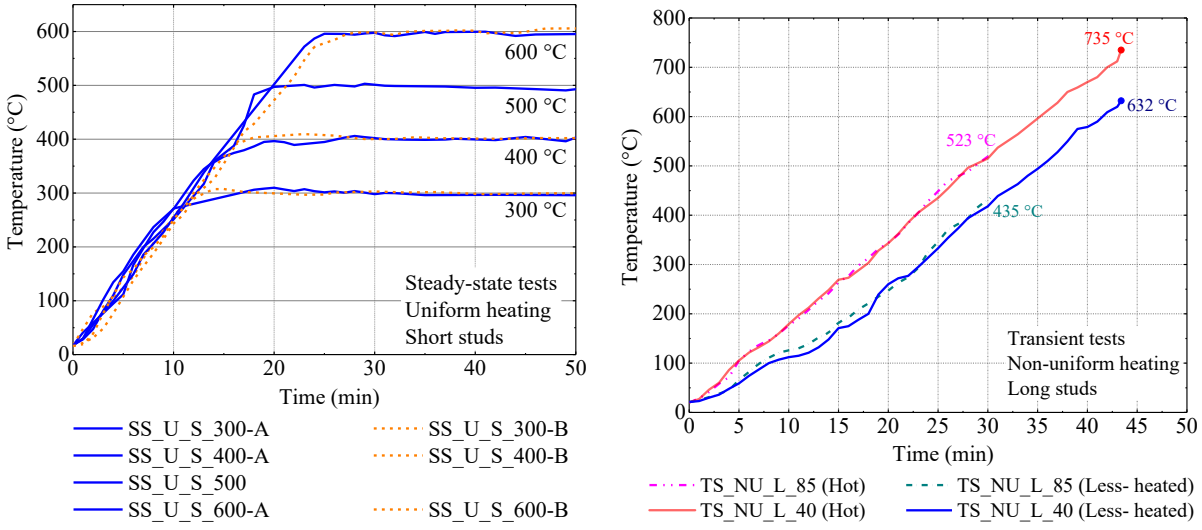

(a) Steady-state tests with uniform heating (b) Transient tests with non-uniform heating

Figure 4: Measured steel temperature on the CFS channel specimens

3. Results

3.1 Steady-state tests

At ambient temperature, the peak axial loads were 101 kN for short studs and 81 kN for long studs. Table 3 summarizes the average peak loads and corresponding strength retention factors obtained from the steady-state tests. When uniformly heated to 400 °C, both short and long studs retained approximately 75% of their ambient-temperature capacities. In contrast, when uniformly heated to 600 °C, the residual capacity of short studs decreased to about 35% of the ambient value, while that of long studs dropped to below 30%.

Table 3: Steady-state tests. Channel average peak loads and retention factors

Stud length / Test conditions	**Short channel studs (457.2 mm)**		**Long channel studs (1219.2 mm)**	
	Peak loads (kN)	Retention factors	Peak loads (kN)	Retention factors
Ambt	101.02	1.000	81.31	1.000
SS_U_300	88.86	0.880	69.79	0.858
SS_NU_300-400	87.70	0.868	74.45	0.916
SS_U_400	77.93	0.771	59.94	0.737
SS_NU_400-500	66.95	0.663	52.18	0.642
SS_U_500	57.69	0.571	32.87	0.404
SS_NU_500-600	40.53	0.401	41.90	0.515
SS_U_600	34.19	0.338	23.71	0.292

Note: SS_U_300 indicates a uniform heating condition in steady-state test with the target temperature of 300 °C, which is the same for SS_U_400, SS_U_500, SS_U_600. SS_NU_300-400 indicates a non-uniform heating condition in steady-state test with the 300 °C at the hot flange and 400 °C at the less-heated flange, which is the same for SS_NU_400-500, SS_NU_500-600.

Under non-uniform heating conditions, higher capacities at elevated temperatures were observed. For example, short and long studs subjected to flange temperature distributions of 500 °C ~ 600 °C retained around 40% and 50% of the ambient capacity, respectively, which were higher than those measured under uniform heating at 600 °C. Similar trends were observed for the non-uniform heating scenarios, where peak loads exceeded those of uniformly heated studs at temperatures equal to the hotter side flange. These results indicate that stud capacity under non-uniform temperature distributions is not governed solely by the maximum flange temperature, but also determined by the flange at less-heated side, with the capacity generally higher than that of uniformly heated studs exposed to the same peak temperature.

Figure 5 shows a sample of load-displacement curves, for short studs under uniform heating. As the stud temperature increases, the peak axial load is reduced.

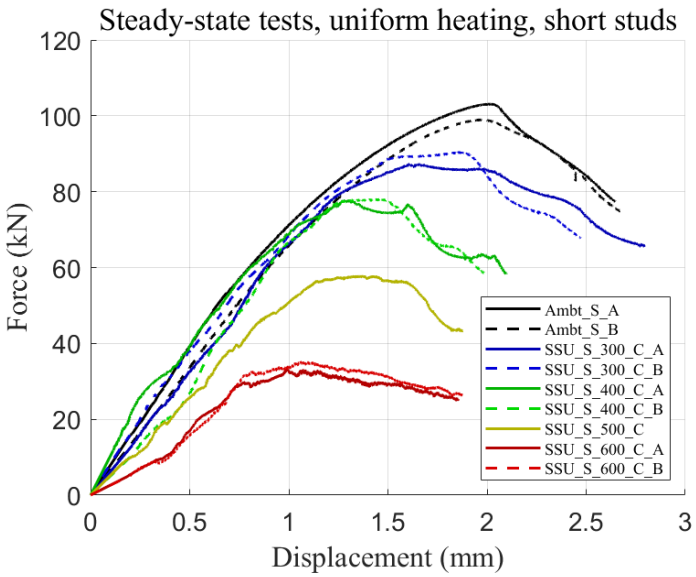

Figure 5: Load-displacement curves for short studs in steady-state tests under uniform temperature

3.2 Transient tests

In transient tests, studs were heated to failure after being loaded to initial utilization ratios of 85% or 40%. During heating, the specimens developed thermal expansion as well as increasing mechanical strains resulting from the (constant) applied load and decreasing mechanical properties. The resulting axial deformations were recorded as displacement-time histories, which can be translated into displacement-temperature histories knowing the heating rate.

shows a sample of results in terms of the measured displacement-temperature curves. The axial displacement initially increased (i.e., expansion) at an approximately constant rate as the temperature increased, before reversing and suddenly contracting at failure. The transient tests showed good repeatability.

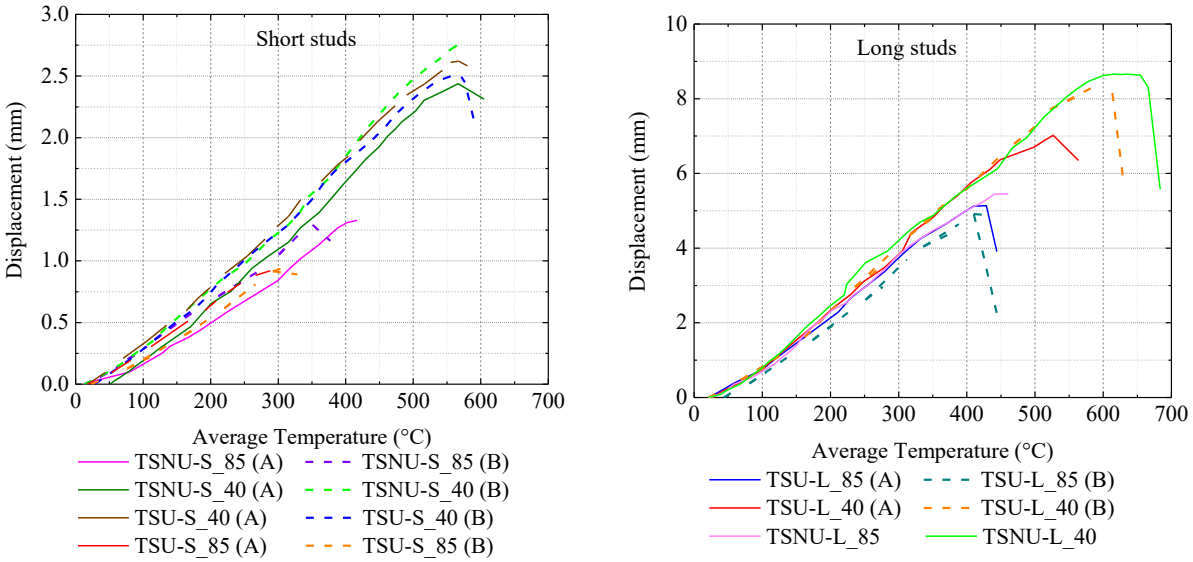

(a) Short studs (b) Long studs

Figure 6: Displacement-average temperature curves for studs in transient tests

Table 4 and Table 5 summarize the critical temperatures (i.e., steel temperatures at failure) obtained from the transient tests, for studs subjected to uniform and non-uniform heating, respectively. For both heating scenarios, studs tested with an initial utilization ratio of 85% failed at lower critical temperatures than those tested at a 40% utilization ratio. In addition, long studs generally failed at higher critical temperatures than short studs under the same loading and heating conditions. For non-uniformly heated studs, the critical temperatures measured at the hot-side flange were higher than those of uniformly heated studs under the same load. This indicates that the behavior of studs under non-uniform temperature distributions is not governed solely by the maximum temperature at the hot-side flange but is also influenced by the less-heated flange.

Table 4: Transient tests, uniform temperature. Channel critical temperatures.

Stud length / Test conditions	**Short channel studs (457.2 mm)**			**Long channel studs (1219.2 mm)**		
	Load (kN)	Heating rate (°C/ min)	Critical temp. (°C)	Load (kN)	Heating rate (°C/ min)	Critical temp. (°C)
TS_U_85-A	85.85	21.84	303	68.24	22.62	444
TS_U_85-B	85.85	22.68	336	68.24	23.20	446
TS_U_40-A	40.39	20.57	592	32.52	22.67	564
TS_U_40-B	40.39	21.69	592	32.52	22.98	630

Table 5: Transient tests, non-uniform temperature. Channel critical temperatures.

Specimen labels	Load (kN)	Heating rate (℃/ min)	Critical temp. (Hot, ℃)	Critical temp. (Less-heated, ℃)
Short channel studs (457.2 mm)				
TS_NU_S_85-A	85.85	18.19	417	314
TS_NU_S_85-B	85.85	17.80	425	330
TS_NU_S_40-A	40.39	16.31	642	569
TS_NU_S_40-B	40.39	17.54	640	560
Long channel studs (1219.2 mm)				
TS_NU_L_85	68.24	15.16	523	435
TS_NU_L_40	32.52	15.28	735	632

3.3 Failure mode

The post-test buckling photos of the studs are shown in Figure 7. Under bearing–bearing boundary conditions, short studs primarily exhibited distortional buckling along the flanges, while local buckling became increasingly pronounced in the flanges and lips as the temperature exceeded 400 °C. Under non-uniform heating, the flanges on the hotter side deformed more significantly than those on the less-heated side. Web buckling in short studs was characterized by one or more buckling waves.

Long studs exhibited a combination of local and distortional buckling. Similar to short studs, local buckling developed on the lips and flanges when the temperature exceeded 400 °C. Some long studs exhibited a single buckling wave along the flanges, whereas others developed two waves. Most specimens displayed symmetric flange buckling, but a few studs exhibited asymmetric flange deformations, preferentially bending in one direction, which was particularly observed under non-uniform heating conditions.

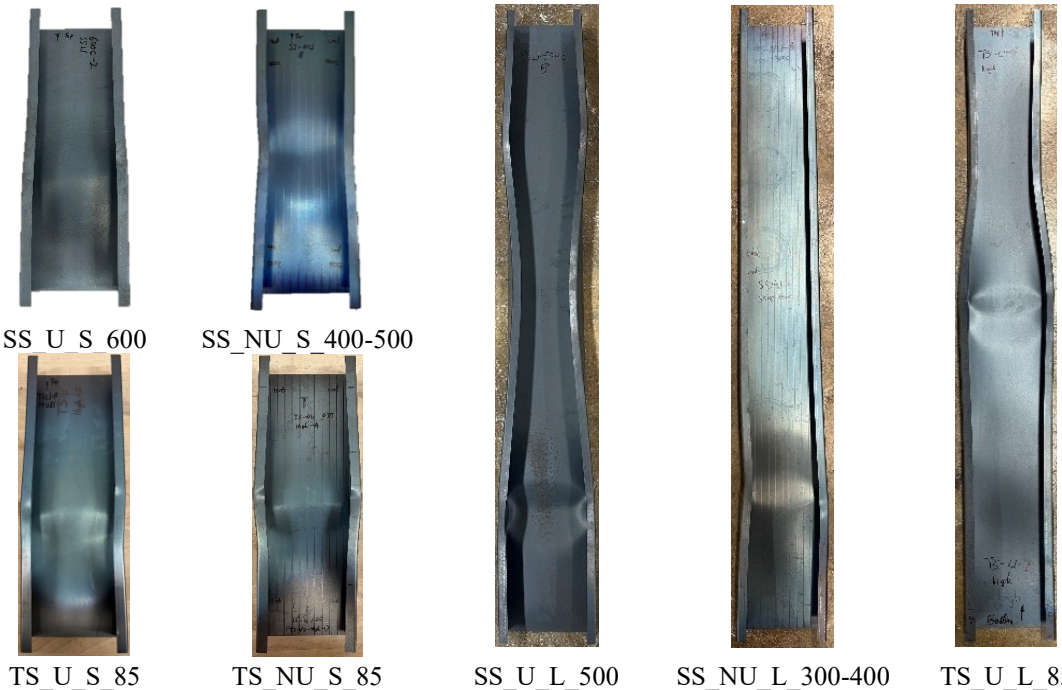

Figure 7: Buckling shape of tested specimens

4. Discussion

Figure 8 plots the test data in terms of axial strength (retention factors) and critical temperatures. The reduction in axial strength with temperature generally aligns with data previously published in the literature for cold-formed steel columns (Xie *et al*. 2025). The data plotted in Figure 8 allows observing the effect of channel length, testing method (steady-state vs. transient testing), and temperature profile (uniform vs. non-uniform temperature), as discussed below.

4.1 Effect of member length

For the steady-state tests, short studs subjected to uniform heating (SS_U_S) exhibited slightly higher retention factors than long studs (SS_U_L). Under non-uniform heating conditions, however, there was no clear trend: while short studs (SS_NU_S) showed slightly higher retention factors than long studs (SS_NU_L) at 400 °C–500 °C temperature distribution, the retention factors of short studs with 300 °C–400 °C and 500 °C–600 °C temperature distributions were lower than those of long studs.

For transient tests under uniform heating, short studs tested at an 85% load ratio exhibited lower critical temperatures than long studs, whereas short and long studs tested at 40% load ratio showed comparable critical temperature, as indicated by TS_U_S and TS_U_L. In contrast, under non-uniform heating conditions, long studs (TS_NU_L) consistently exhibited higher critical temperatures than short studs (TS_NU_S).

4.2 Effect of testing method

The data from steady-state tests and transient tests are compared herein. For specimens under uniform elevated temperature, the response of short studs is very consistent between the steady-state and the transient tests. Indeed, the retention factors of short studs in steady-state tests closely correspond to the load ratios of short studs in transient tests that failed at similar critical temperatures, as indicated by SS_U_S and TS_U_S in Figure 8. A similar trend is observed for long studs; however, long studs with comparable critical temperatures exhibited lower retention factors in the steady-state tests than the corresponding load ratios measured in the transient tests (SS_U_L and TS_U_L).

Under non-uniform heating, for short studs (SS_NU_S and TS_NU_S), the critical temperatures measured in transient tests at an 85% load ratio closely match the preheating temperatures of short studs tested at 300–400 °C in the steady-state tests. At a 40% load ratio, the transient test critical temperatures were approximately 50 °C higher than the corresponding preheating temperatures for studs with retention factors near 40% in the steady-state tests. For long studs (SS_NU_L and TS_NU_L), however, critical temperatures recorded in transient tests were consistently higher than the preheating temperatures of studs failing at comparable retention factors that were closed to 85% and 40% in the steady-state tests. This indicates that, whereas the capacity and critical temperature of short studs are almost insensitive to the test methods, long studs exhibit higher critical temperatures in transient tests than in steady-state tests under comparable thermal and loading conditions.

4.3 Effect of temperature distribution

For short studs, in steady-state tests, the strength under non-uniform temperature fell in between the strengths under uniform temperature equal to the hotter-side and less-heated flange

temperatures. The retention factors of non-uniformly heated short studs in steady-state tests (SS_NU_S) were higher than those of studs uniformly heated to the hotter side flange temperature, but lower than those of studs uniformly heated to the less-heated flange temperature (SS_U_S). This indicates that the failure of short studs with a 100 °C cross-sectional gradient is not governed solely by the hotter side temperature, the thermal condition of the less-heated side also plays a significant role.

Despite a similar behavior was observed for long studs heated to 400 °C–500 °C, long studs with 300 °C–400 °C and 500 °C–600 °C temperature distribution failed with retention factors exceeding those of studs uniformly heated to the less-heated side temperature, as illustrated through SS_NU_L and SS_U_L in Figure 8.

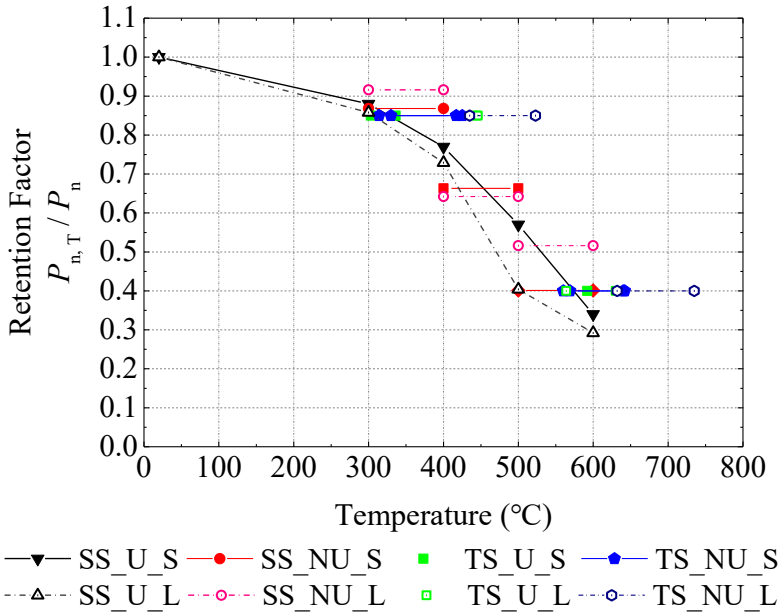

Figure 8: Relationship between normalized axial strength and temperature for the cold-formed steel lipped channels in compression. Data from steady-state and transient tests under uniform and non-uniform heating.

In transient tests, considering the same load ratios, uniformly heated short studs failed at the critical temperatures that were close to the critical temperatures at the less-heated side of short studs subjected to non-uniform heating, as indicated by TS_NU_S and TS_U_S. However, for long studs, the temperatures at the less-heated side under non-uniform heating exceeded the critical temperatures of long studs under uniform heating, as shown by with TS_NU_L and TS_U_L. These findings again suggest that the failure of non-uniform heated studs is governed not only by hotter side flanges but also by the thermal conditions of less-heated-side flanges.

5. Conclusion

This study investigates the compressive strength and buckling behavior of short and long 600S200-54 cold-formed steel lipped channel members subjected to uniform and non-uniform elevated temperatures under steady-state and transient heating. Using a custom-built electrical furnace, controlled temperature histories and flange temperature gradients representative of fire conditions were applied to axially loaded cold-formed steel members. In the steady-state tests,

specimens were exposed to temperatures up to 600 °C, including a temperature gradient of 100 °C between flanges, while transient tests were performed under applied load ratios of 40% and 85%.

The steady-state tests showed that member strength decreased to approximately 75% of ambient capacity at 400 °C and to about 30% at 600 °C, with failure governed by local and distortional buckling of the flanges, lips, and webs. Transient tests showed the strong dependence of failure temperature on load ratio, as specimens loaded to 85% of their ambient capacity failed between 300 °C and 450 °C, whereas those loaded to 40% sustained temperatures close to 600 °C. Transient tests were generally consistent with the steady-state test results, but differences between short and long members were observed, with long specimens exhibiting higher capacities under transient heating than in corresponding steady-state tests.

Tests with non-uniform heating showed that failure was not governed solely by the temperature of the hotter flange; the contribution of the cooler flange played a significant role in strength. Indeed, under non-uniform heating, the hotter flange temperature at failure generally exceeded the critical temperature under uniform heating conditions.

These results provide new member-level experimental data under transient and non-uniform thermal conditions and offer benchmarks for the calibration and validation of analytical and numerical models. These data and models support the development of performance-based fire design methods for cold-formed steel structures.

Acknowledgments
This material is based upon work supported by the U.S. National Science Foundation (NSF) under award No. 2237623 "CAREER: Performance-Based Fire Design for Cold-Formed Steel Structures" (PI T. Gernay). The financial support is gratefully acknowledged.

The authors are thankful to Unarco Material Handling, Inc. and to Jim Crews for the donation and transport of the lipped channels.

References

Abreu, J. C. B., Vieira Jr, L. C., Moreno Jr, A. L., Gernay, T., & Schafer, B. W. (2020). "Experiments on load-bearing cold-formed steel sheathed studs at elevated temperatures." *Thin-Walled Structures*, 156, 106968.

Ali, F. A., Shepherd, P., Randall, M., Simms, I., O'Connor, D. J., & Burgess, I. (1998). "The effect of axial restraint on the fire resistance of steel columns." *Journal of Constructional Steel Research*, 46, 305-306.

Ariyanayagam, A., & Mahendran, M. (2014). "Experimental study of load-bearing cold-formed steel walls exposed to realistic design fires." *Journal of Structural Fire Engineering*, 5(4), 291-330.

ASTM E21, West Conshohocken, (2009). "ASTM E21, Standard Test Methods for Elevated Temperature Tension Tests of Metallic Materials." *American Society for Testing and Materials*.

ASTM E8, International, West Conshohocken, (2016). "ASTM E8/ E8M-16, Standard Test Methods for Tension Testing of Metallic Materials.", *West Conshohocken, PA, USA: ASTM International*.

CFS-NHERI: 10-Story Building Capstone Test Program. University of California San Diego, Johns Hopkins University, California Polytechnic State University, San Luis Obispo, University of Massachusetts Amherst. (2025) https://cfs10.ucsd.edu/ (accessed October 29, 2025).

Chen, W., Ye, J., Bai, Y., & Zhao, X. L. (2012). "Full-scale fire experiments on load-bearing cold formed steel walls lined with different panels." *Journal of Constructional Steel Research*, 79, 242-254.

Craveiro, H. D., Rodrigues, J. P. C., & Laím, L. (2016) "Experimental analysis of built-up closed cold-formed steel columns with restrained thermal elongation under fire conditions." *Thin-Walled Structures*, 107, 564-579.

David C. Fratamico, Shahabeddin Torabian, Xi Zhao, Kim J.R. Rasmussen, Benjamin W. S. (2018). "Experimental study on the composite action in sheathed and bare built-up cold-formed steel columns." *Thin-Walled Structures*, 127, 290-305.

Dias, Y., Mahendran, M., & Poologanathan, K. (2019). "Full-scale fire resistance tests of steel and plasterboard sheathed web-stiffened stud walls". *Thin-Walled Structures*, 137, 81 93.

Feng, M., & Wang, Y. C. (2005), "An experimental study of loaded full-scale cold-formed thin walled steel structural panels under fire conditions." *Fire Safety Journal*, 40(1), 43 63.

Feng, M., Wang, Y. C., & Davies, J. M. (2003). "Structural behaviour of cold-formed thin-walled short steel channel columns at elevated temperatures. Part 1: experiments." *Thin-walled structures*, 41(6), 543-570.

Gunalan, S., Heva, Y. B., & Mahendran, M. (2015). "Local buckling studies of cold-formed steel compression members at elevated temperatures." *Journal of Constructional Steel Research*, 108, 31-45.

Kesawan, S., & Mahendran, M. (2015) "Fire tests of load-bearing LSF walls made of hollow flange channel sections". *Journal of Constructional Steel Research*, 115, 191-205.

Liu, K., Chen, W., Ye, J., Jiang, J., Fang, Z., & Lim, J. B. (2024). "Fire performance enhancement of cold-formed steel walls: experimental and numerical study." *Engineering Structures*, 314, 118419.

Ma, C., Yan X., and Thomas G. (2025). "Properties of cold-formed steels exposed to elevated temperatures. Construction Materials and Their Properties for Fire Resistance and Insulation." *Woodhead Publishing*, 2025. 59-78.

Ranawaka, T., & Mahendran, M. (2009). "Distortional buckling tests of cold-formed steel compression members at elevated temperatures." *Journal of Constructional Steel Research*, 65(2), 249-259.

Roy, K., Lim, J. B., Lau, H. H., Yong, P. M., Clifton, G. C., Johnston, R. P., Wrzesien, A., & Mei, C. C. (2019). "Collapse behaviour of a fire engineering designed single-storey cold-formed steel building in severe fires." *Thin-Walled Structures*, 142, 340-357.

Roy, K., Ting, T. C. H., Lau, H. H., & Lim, J. B. (2019). "Experimental and numerical investigations on the axial capacity of cold-formed steel built-up box sections." *Journal of Constructional Steel Research*, 160, 411-427.

Samiee, P., Niari, S. E., & Ghandi, E. (2022). "Thermal and structural behavior of cold-formed steel frame wall under fire condition." *Engineering Structures*, 252, 113563.

Tian, Y. S., Wang, J., Lu, T. J., & Barlow, C. Y. (2004). "An experimental study on the axial behaviour of cold-formed steel wall studs and panels." *Thin-walled structures*, *42*(4), 557-573.

Vieira Jr, L. C. M., Shifferaw, Y., & Schafer, B. W. (2011). "Experiments on sheathed cold-formed steel studs in compression". *Journal of Constructional Steel Research*, 67(10), 1554-1566.

Xie, J., Niu, Y., & Gernay, T. (2025). "Experiments on local buckling of cold-formed steel lipped channels in compression at elevated temperatures." *Engineering Structures*, 338, 120594.

Xie, J., & Gernay, T. (2025). "Steady-state elevated temperature tests on cold-formed steel channels with uniform heating. Experiments on cold-formed steel lipped channels in compression at elevated temperatures". *DesignSafe-CI*. https://doi.org/10.17603/ds2-z01a-nz04.

Xie, J., Schafer, B. W., & Gernay, T. (2025). "A review of experiments on cold-formed steel members at elevated temperatures." *Journal of Constructional Steel Research*, 229, 109482.

Yang, J., Zhou, X., Wang, W., Xu, L., & Shi, Y. (2023). "Fire resistance of box-shape cold-formed steel built-up columns failing in global buckling: Test, simulation and design". *Thin-Walled Structures*, 183, 110433.

Yap, D. C., & Hancock, G. J. (2011). "Experimental study of high-strength cold-formed stiffened-web C-sections in compression." *Journal of Structural Engineering*, 137(2), 162-172.

Zhang, Z., Singh, A., Speicher, M. S., Peterman, K. D., Hutchinson, T. C., & Schafer, B. W. (2025). "Modeling cold-formed steel framed wall-lines with steel sheet sheathed shear walls." *Thin-Walled Structures*, 113408.